

## Reducing the reflection error of PML absorbing boundary conditions within a generalized Maxwell-Bloch framework

Johannes Popp\*, Lukas Seitner, Michael Haider, and Christian Jirauschek  
 Department of Electrical and Computer Engineering, Technical University of Munich,  
 Arcisstr. 21, 80333 Munich, Germany

### Abstract

We demonstrate a full-wave numerical Maxwell-Bloch simulation tool including perfectly matched layer (PML) absorbing boundary conditions. To avoid detrimental reflection errors at the boundary of the simulation domain, an adapted PML model is introduced, which takes into account impedance mismatch effects arising from the internal quantum system. For the numerical validation of the modified PML model the simulation tool is applied to the active gain medium of a terahertz quantum cascade laser (QCL) structure. Improved absorbing characteristics for the truncation of active gain media in our Maxwell-Bloch simulation approach are obtained.

### 1 Introduction

The Maxwell-Bloch equations are a valuable tool for modeling light-matter interaction in nonlinear optics [1, 2]. Here, the evolution of a discrete-level quantum system is described by the Bloch equations, which are coupled to Maxwell's equations and provide a classical description of the optical field. In recent years, this equation system has been applied to the simulation of various active photonic devices in order to describe nonlinear optical phenomena [3–9]. The work presented here is based on the open-source solver tool *mbsolve* [10, 11], where the generalized one-dimensional Maxwell-Bloch equations are treated without invoking the rotating wave approximation (RWA).

In order to solve the Maxwell-Bloch equations, *mbsolve* uses the finite-difference time-domain (FDTD) method, one of the standard approaches in computational electrodynamics [12]. A main challenge in simulating optical devices in open radiation problems is the truncation of the FDTD lattice [12]. Here, the main idea is to introduce a highly absorbing, reflectionless layer at the outer boundary of the spatial FDTD grid. In 1994, Berenger introduced perfectly matched layers as a non-physical absorber [13]. His approach is based on the so called field-splitting method, where the field components are split into two orthogonal compo-

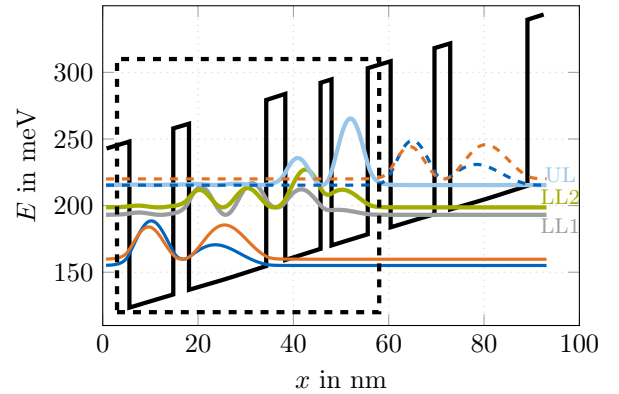


**Figure 1.** Calculated conduction band profile and probability densities of the investigated THz QCL structure [8, 19] with an optical transition frequency of 3.5 THz. The upper and lower laser levels are represented by bold solid lines. The dashed rectangle comprises a single QCL period.

nents resulting in modified Maxwell's equations. Based on this work, Fang *et al.* [14, 15] introduced a general PML method for lossy materials by extending the original PML approach by Berenger. A uniaxial anisotropic PML (UPML) absorber was introduced by Gedney [16], where the mathematical model of field-splitting is replaced by a more physical model based on the Maxwellian formulation. In a consecutive publication, he extended his approach for the absorption of fields in lossy and dispersive materials [17]. Wang *et al.* [18] presented a PML approach for the truncation of a gain medium within a semiconductor Maxwell-Bloch framework for both, un-split and field-splitting methods.

In this paper, we introduce the theoretical model for the integration of UPML boundary conditions into the existing code base of *mbsolve*. For the evaluation of the PML implementation we will use a well-studied quantum cascade laser design [8, 19] as an exemplary device. A QCL is a special type of semiconductor laser emitting in the mid-infrared and THz frequency range. Its active gain medium consists of a multiple quantum well heterostructure. Quantized electron states act as

laser levels and charge transport occurs through inter-subband transitions between the states [20]. In Fig. 1, the bandstructure and calculated wavefunctions of the investigated THz QCL gain medium are illustrated. Optical transitions appear between the upper level UL and the two lower levels LL1 and LL2. All relevant simulation parameters can be found in [11].

## 2 Simulation model

The Maxwell-Bloch equations describe the light-matter interaction of the optical field with a quantum mechanical system. The density operator  $\hat{\rho}(t, x)$  contains all information about the quantized electronic states. In order to minimize the workload for the numerical simulations, we reduce the model to a single spatial coordinate. The validity of this simplification is guaranteed as we restrict our investigations to optoelectronic devices with widespread waveguides in propagation and lateral direction, thus allowing the separation of the electromagnetic field into transverse and longitudinal modes [2]. In the following, the propagation direction is  $x$  and the optical field is represented by the field components  $E_z(x, t)$  and  $H_y(x, t)$  with  $z$  and  $y$  being the transversal coordinates. The density operator  $\hat{\rho}(t, x)$  is governed by the Liouville-von Neumann master equation

$$\partial_t \hat{\rho} = -i\hbar^{-1} [\hat{H}_0 - \hat{\mu}_z E_z, \hat{\rho}] + \mathcal{D}(\hat{\rho}), \quad (1)$$

where  $\hbar$  is the reduced Planck constant,  $\hat{H}_0$  is the system Hamiltonian,  $\hat{\mu}_z$  is the dipole moment operator, and  $[\cdot, \cdot]$  denotes the commutator  $[\hat{A}, \hat{B}] = \hat{A}\hat{B} - \hat{B}\hat{A}$ . The dissipation superoperator  $\mathcal{D}(\hat{\rho})$  models the interaction with the environment. From the dipole moment of the quantum system the macroscopic polarization term  $P_{z,\text{qm}}$  is obtained by

$$P_{z,\text{qm}} = n_{3\text{D}} \text{Tr}\{\hat{\mu}_z \hat{\rho}\}, \quad (2)$$

where  $n_{3\text{D}}$  is the carrier number density.

The optical field propagation is described classically using Faraday's law and Ampere's law for the electric field  $E_z$  and magnetic field  $H_y$ . By utilizing the auxiliary differential equation approach the update equations in the UPML medium can be derived. Using the relation  $D_z(\omega) = \varepsilon_0 \varepsilon_r(\omega) E_z(\omega)$  and taking into account the constitutive parameter  $s_x = 1 + \frac{\sigma_x}{i\omega \varepsilon_0}$ , the time evolution equation for the electric flux density is given by

$$\partial_t D_z = \partial_x H_y - \frac{\sigma_x}{\varepsilon_0} D_z, \quad (3)$$

with the UPML conductivity  $\sigma_x$ . Furthermore, the time evolution of the electric field is represented by

$$\partial_t E_z = (\varepsilon_0 \varepsilon_{r,\infty})^{-1} \left( \partial_t D_z - \sigma_0 E_z - \partial_t P_{z,\text{qm}} - \sum_i \partial_t P_{z,\text{class}}^i \right), \quad (4)$$

where  $\varepsilon_0 \varepsilon_{r,\infty}$  is the product of the vacuum permittivity and the relative permittivity in the infinite-frequency limit,  $\sigma_0$  is the material conductivity and  $\sum_i \partial_t P_{z,\text{class}}^i$  is the multi-polarization term accounting for bulk and waveguide dispersion [12]. We also take into account the macroscopic polarization of the quantum system in the PML in order to reduce the reflection error at the interface layer between the absorbing boundary and the main simulation region. Several generic models such as e.g. Drude and Lorentz are implemented and can be combined. The time evolution equation of the magnetic field can be written as

$$\partial_t H_y = \mu^{-1} \partial_x E_z - \frac{\sigma_x}{\varepsilon_0} H_y, \quad (5)$$

with the permeability  $\mu = \mu_0 \mu_r$ . In order to reduce the parasitic reflection errors from the PML layers, the conductivity  $\sigma_x$  in the PML layers is gradually increased along the propagation direction. Therefore, the conductivity is varied using a smooth polynomial with depth  $x$  in the PML layer [12, 16]

$$\sigma_x(x) = (x/d)^m \sigma_{x,\text{max}}. \quad (6)$$

The optimal choice for  $\sigma_{x,\text{max}}$  is given by [12, 17]

$$\sigma_{x,\text{opt}} = \frac{0.8(m+1)}{\eta_0 \Delta \sqrt{\varepsilon_{r,\text{eff}} \mu_{r,\text{eff}}}}, \quad (7)$$

where  $\eta_0$  is the free-space wave impedance,  $\Delta$  is the lattice-cell dimension, and  $\varepsilon_{r,\text{eff}}$  and  $\mu_{r,\text{eff}}$  are constants representing the effective relative permittivity and permeability, respectively. The values of  $\varepsilon_{r,\text{eff}}$  and  $\mu_{r,\text{eff}}$  should be chosen either to be mean values of the physical parameters or the values at the wavenumber of the fundamental mode in the waveguide [12].

## 3 Results

We validate the numerical stability of our modified PML model by investigating the light propagation in the aforementioned THz QCL gain structure for two different simulation setups, as depicted in Fig. 2. Setup 1 consists of an active region of length 5 mm, which is terminated by a perfect magnetic conductor (PMC) layer on the left and a 200-layer PML region on the right facet. Setup 2 has a simulation domain twice as long as in setup 1 and is terminated with a PMC boundary layer on both sides.

As pointed out in [11], the chromatic dispersion in the investigated THz structure arises not only from the quantum system, but also from the background material and the waveguide itself. Here, the chromatic dispersion introduced by the background system is neglected, as we are more interested in the interaction of the PML region with the quantum system. In order to extract the spectral gain profile we excite the system with a Gaussian field pulse  $E_z(0, t) =$

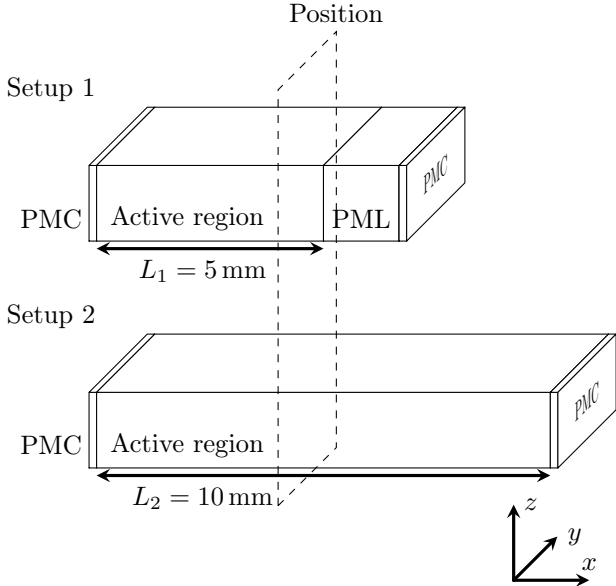


**Figure 2.** Illustration of the two different simulation setups under numerical investigation. Setup 1 describes a THz gain medium with length  $L_1 = 5$  mm truncated with a PML boundary containing 200 grid-points terminated by a PMC layer, setup 2 is based on the same material system with twice the length and two PMC layers at the facets.

A  $\exp[-(t - t_0)/\tau]^2 \sin(2\pi f_0 t)$  at the left facet of setup 1 and measure the amplified field at the position  $x = L = 4$  mm, indicated by a dashed rectangle in Fig. 2. The pulse parameters are  $A = 1 \times 10^{-3}$  V/m,  $\tau = 0.707$  ps,  $t_0 = 30$  ps, and  $f_0 = 3.8$  THz. The amplitude gain coefficient can be calculated from the Fourier transforms of the recorded electric fields  $E_{\text{in}}(\omega)$  and  $E_{\text{out}}(\omega)$  by

$$g(\omega) = \frac{1}{L} \ln \left( \frac{|E_{\text{out}}(\omega)|}{|E_{\text{in}}(\omega)|} \right). \quad (8)$$

The resulting spectral gain profile of the THz QCL gain medium is presented in Fig. 3. We observe two gain peaks at  $f = 3.63$  THz and  $f = 4.13$  THz which correspond to the optical transitions  $\text{UL} \rightarrow \text{LL2}$  and  $\text{UL} \rightarrow \text{LL1}$ , respectively. Our simulation yields a peak gain of  $g_p = 19.7 \text{ cm}^{-1}$ .

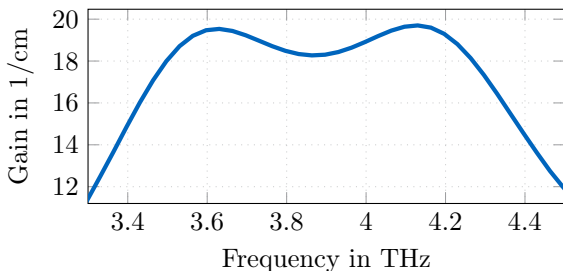


**Figure 3.** Simulated spectral gain profile of the THz QCL gain structure.

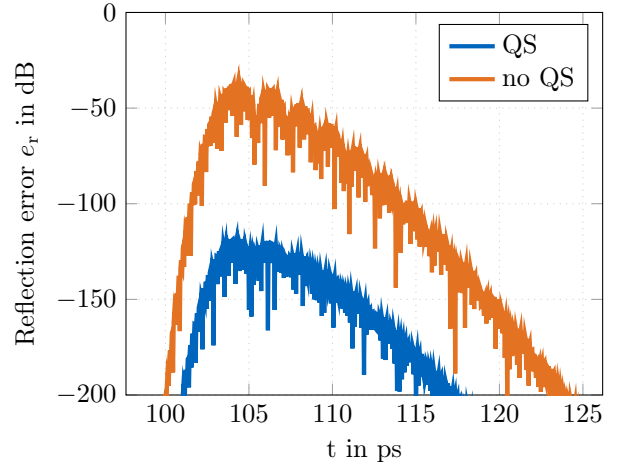


**Figure 4.** Reflection error for two PML configurations. The blue curve represents the reflection error including the macroscopic polarization of the QS in the PML region, whereas the orange curve represents the results obtained from the original PML formulation introduced by Gedney [16, 17].

We now quantify the reflection behavior at the PML boundary by introducing the reflection error  $e_r$ , computed as

$$e_r(t) = \frac{|E_1(t) - E_2(t)|}{\max(|E_2(t)|)} \Big|_{x=4\text{mm}}, \quad (9)$$

with  $E_1(t)$  being the reflected electric field in setup 1. The field  $E_2(t)$  from setup 2 is used as reference value. As already pointed out, we also include the quantum system of the active region in the adjacent PML region to obtain better impedance matching. The amplitude gain displayed in Fig. 3 now also acts on the outgoing electric field in the PML. However, the artificially introduced losses from Eq. (6) outperform the unintended amplification by far and the light gets efficiently absorbed in the PML region. In Fig. 4, we compare the results of our implementation to a similar PML region, but here we drop the quantum system (QS) in the boundary. Due to the resulting impedance mismatch such a scenario yields a maximum reflection error of  $e_r \sim -36$  dB for the exemplary THz QCL setup. By taking into account the QS in the PML layers, we obtain a reflection error  $e_r$  of less than  $-118$  dB.

## 4 Conclusion

In this paper, we presented an extension to the existing generalized open source Maxwell-Bloch equation framework with the incorporation of perfectly matched layer absorbing boundary conditions. By applying the new implementation to a THz QCL gain medium an efficient attenuation of outwards propagating fields has been demonstrated. We integrate the quantum gain system into the PML region and thus assure an improved outcoupling of the optical field. A significantly

reduced reflection error as compared to previous PML models has been achieved.

## 5 Acknowledgements

The authors acknowledge financial support by the European Union's Horizon 2020 research and innovation programme under grant agreement No 820419 – Qombs Project "Quantum simulation and entanglement engineering in quantum cascade laser frequency combs" (FET Flagship on Quantum Technologies).

## References

- [1] R. W. Boyd, *Nonlinear Optics*, 4th ed. Academic Press, 2020.
- [2] C. Jirauschek, M. Riesch, and P. Tzenov, "Optoelectronic device simulations based on macroscopic Maxwell-Bloch equations," *Adv. Theory Simul.*, vol. 2, no. 8, p. 1900018, 2019.
- [3] G. Slavcheva, J. M. Arnold, I. Wallace, and R. W. Ziolkowski, "Coupled Maxwell-pseudospin equations for investigation of self-induced transparency effects in a degenerate three-level quantum system in two dimensions: Finite-difference time-domain study," *Phys. Rev. A*, vol. 66, p. 063418, 2002.
- [4] G. Slavcheva, "Model for the coherent optical manipulation of a single spin state in a charged quantum dot," *Phys. Rev. B*, vol. 77, p. 115347, 2008.
- [5] C. R. Menyuk and M. A. Talukder, "Self-induced transparency modelocking of quantum cascade lasers," *Phys. Rev. Lett.*, vol. 102, p. 023903, 2009.
- [6] M. A. Talukder and C. R. Menyuk, "Quantum coherent saturable absorption for mid-infrared ultrashort pulses," *Opt. Express*, vol. 22, no. 13, pp. 15 608–15 617, 2014.
- [7] R. W. Ziolkowski, J. M. Arnold, and D. M. Gogny, "Ultrafast pulse interactions with two-level atoms," *Phys. Rev. A*, vol. 52, pp. 3082–3094, 1995.
- [8] P. Tzenov, D. Burghoff, Q. Hu, and C. Jirauschek, "Time domain modeling of terahertz quantum cascade lasers for frequency comb generation," *Opt. Express*, vol. 24, no. 20, pp. 23 232–23 247, 2016.
- [9] C. Jirauschek and P. Tzenov, "Self-consistent simulations of quantum cascade laser structures for frequency comb generation," *Opt. Quant. Electron.*, vol. 49, no. 12, p. 414, 2017.
- [10] M. Riesch and C. Jirauschek, "mbsolve: An open-source solver tool for the Maxwell-Bloch equations," *Comput. Phys. Commun.*, vol. 268, p. 108097, 2021.
- [11] L. Seitner, J. Popp, M. Riesch, M. Haider, and C. Jirauschek, "Group velocity dispersion in terahertz frequency combs within a generalized Maxwell-Bloch framework," *J. Phys.: Conf. Ser.*, vol. 2090, no. 1, p. 012082, 2021.
- [12] A. Taflov and S. C. Hagness, *Computational Electrodynamics: The Finite-Difference Time-Domain Method*, 3rd ed. Artech House, Boston, 2005.
- [13] J.-P. Berenger, "A perfectly matched layer for the absorption of electromagnetic waves," *J. Comp. Phys.*, vol. 114, no. 2, pp. 185–200, 1994.
- [14] J. Fang and Z. Wu, "Generalized perfectly matched layer—an extension of Berenger's perfectly matched layer boundary condition," *IEEE Microwave Guided Wave Lett.*, vol. 5, no. 12, pp. 451–453, 1995.
- [15] —, "Generalized perfectly matched layer for the absorption of propagating and evanescent waves in lossless and lossy media," *IEEE Trans. Microwave Theory Tech.*, vol. 44, no. 12, pp. 2216–2222, 1996.
- [16] S. D. Gedney, "An anisotropic perfectly matched layer-absorbing medium for the truncation of FDTD lattices," *IEEE Trans. Antennas and Propag.*, vol. 44, no. 12, pp. 1630–1639, 1996.
- [17] —, "An anisotropic PML absorbing media for the FDTD simulation of fields in lossy and dispersive media," *Electromagnetics*, vol. 16, no. 4, pp. 399–415, 1996.
- [18] Q. Wang and S.-T. Ho, "Implementation of perfectly matched layer boundary condition for finite-difference time-domain simulation truncated with gain medium," *J. Lightwave Technol.*, vol. 29, no. 10, pp. 1453–1459, 2011.
- [19] D. Burghoff, T.-Y. Kao, N. Han, C. W. I. Chan, X. Cai, Y. Yang, D. J. Hayton, J.-R. Gao, J. L. Reno, and Q. Hu, "Terahertz laser frequency combs," *Nat. Photonics*, vol. 8, no. 6, pp. 462–467, 2014.
- [20] C. Jirauschek and T. Kubis, "Modeling techniques for quantum cascade lasers," *Appl. Phys. Rev.*, vol. 1, no. 1, p. 011307, 2014.